24th COBEM - 2017

24th ABCM International Congress of Mechanical Engineering
December 3-8, 2017, Curitiba, PR, Brazil

COBEM-2017-1594
SHEAR-INDUCED HYDRODYNAMIC DIFFUSION AND AGGREGATION IN NON-BROWNIAN DILUTE MAGNETIC SUSPENSIONS

Gesse A. Roure Neto
Francisco R. Cunha
Universidade de Brasília, Department of Mechanical Engineering, VORTEX Group, Brasília, Brasil
gesse.roure@gmail.com , frcunha@unb.br

Abstract. *In recent years, magnetic suspensions have found a number of applications in engineering. These applications are mainly due to the fact that the rheological properties of these suspensions change in the presence of an external field. In this paper we use a two-particle model in order to study transport phenomena on magnetic suspensions, like shear induced hydrodynamic diffusion and shear-induced aggregation in the regime of large Péclet numbers. In this model, we consider two identical particles free of inertia in creeping flow regime undergoing an external simple shear in the presence of dipole-dipole magnetic interactions and viscous hydrodynamic interactions between the two particles. For the numerical computation of the relative particle trajectories, we use a fourth order Runge-Kutta scheme with adaptive time step. In order to investigate the interplay between aggregative and dispersive trajectories, we use scatter diagrams to show the end position of particles coming from a starting plane and sections of a basin of aggregation to show the aggregative area given an initial configuration and the position of the starting plane of particles. In addition, we also calculate the hydrodynamic self-diffusivity, down-gradient diffusivity and the rate of particle doublet formation resulting from aggregative trajectories. The numerical computation of the diffusivities and aggregation rates are performed by the use of a Monte-Carlo integration for different values of the magnetic parameter α, which represents the non-dimensional strength of the dipole-dipole magnetic interactions. For small values of α, it was possible to fit the results for the self-diffusivity in a curve similar to the asymptotic curve for small values of roughness (Cunha and Hinch, 1996). Finally, based on physical scaling arguments we propose a theory that predicts a power law dependence of the rate of aggregation as a function of the dipole interaction parameter α. These theories show good agreement with the simulation results.*

Keywords: *Magnetic suspensions , dipole-dipole interaction, hydrodynamic interactions , shear-induced diffusivity , shear-induced aggregation*

1. INTRODUCTION

In recent years, magnetic suspensions have found a large number of applications in engineering, including hard drive seals, magnetorheological dumpers, shock absorbers, clutches and medical applications. Ferrofluids and magnetorheological suspensions are very useful due to the fact that their properties change in the presence of an external field, allowing a certain level of control of those properties.

Two-particle dynamics have been used for a long time in order to predict macroscopic transport properties of suspensions. The classical paper by Batchelor (Batchelor and Green, 1972) uses the dynamic of two particles and the solution for the pair distribution function in order to calculate the term of order ϕ^2 of the stress tensor in a suspension.

The relative motion of two colliding spherical particles free of inertia in Stokes flow is reversible due to the linearity of the Stokes equation. The effect of hydrodynamic diffusion is due to the symmetry breaking on particle collisional relative trajectories due to some parameter, like particle roughness (Cunha and Hinch, 1996), the non-sphericity of the particles, deformability (Loewenberg and Hinch, 1997), field interacions between the particles (Cunha and Couto, 2008; Cunha *et al.*, 2013) or the presence of a third particle. Unlike Brownian diffusion, the hydrodynamic diffusion depends on the concentration of particles. Shear-induced hydrodynamic diffusion has been a topic of interest more recently due to a wide range of applications in many practical problem of interest occurring in the mycrohydrodynamical scale instead of the molecular one. For instance, this includes from aggregation-flocculation of suspended particles to mixing-diffusion and migration of cells in blood flows (Grandchamp *et al.*, 2013).

The formation of particle aggregates is an intrinsic phenomenon in magnetic suspensions, as a result of the attractive dipolar forces between the particles. In the present context, when particles are brought close together by the flow, the magnetic dipole-dipole interactions being attractive may result in particle aggregation. The two-particle model developed here with particles interacting magnetically and hydrodynamically gives the relative particle trajectories for several initial particle configurations. From the trajectory calculation, we can also predict the rate of doublet formation in a dilute

magnetic suspension undergoing a shear flow.

2. COMPUTATIONAL PROCEDURE

The governing equations for the motion of the particles are given by:

$$\frac{d\boldsymbol{x}_i}{dt} = \boldsymbol{U}_i \tag{1}$$

and

$$\frac{d\hat{\boldsymbol{p}}_i}{dt} = \boldsymbol{\omega}_i \wedge \hat{\boldsymbol{p}}_i, \tag{2}$$

where $\boldsymbol{x}_i$ and $\boldsymbol{U}_i$ denotes particle position and velocity, respectively. $\hat{\boldsymbol{p}}_i$ is an unit vector representing the particle-dipole orientation and $\boldsymbol{\omega}_i$ is the particle angular velocity. As the main interest here is to calculate the net displacement of a particle across its original streamline, it is more appropriated to focus on the analysis of the particle relative trajectories, i.e. $\boldsymbol{r} = \boldsymbol{x}_2 - \boldsymbol{x}_1$. In the absence of inertia and Brownian motion, the translational and rotational velocities of the two particles are given by Kim and Karrila (2013):

$$\begin{bmatrix} \boldsymbol{u}^\infty(\boldsymbol{x}_1) - \boldsymbol{U}_1 \\ \boldsymbol{u}^\infty(\boldsymbol{x}_2) - \boldsymbol{U}_2 \\ \boldsymbol{\Omega}^\infty(\boldsymbol{x}_1) - \boldsymbol{\omega}_1 \\ \boldsymbol{\Omega}^\infty(\boldsymbol{x}_1) - \boldsymbol{\omega}_2 \end{bmatrix} = \begin{bmatrix} \boldsymbol{a}_{11} & \boldsymbol{a}_{12} & \tilde{\boldsymbol{b}}_{11} & \tilde{\boldsymbol{b}}_{12} & \tilde{\boldsymbol{g}}_1 \\ \boldsymbol{a}_{21} & \boldsymbol{a}_{22} & \tilde{\boldsymbol{b}}_{21} & \tilde{\boldsymbol{b}}_{22} & \tilde{\boldsymbol{g}}_2 \\ \boldsymbol{b}_{11} & \boldsymbol{b}_{12} & \boldsymbol{c}_{11} & \boldsymbol{c}_{12} & \tilde{\boldsymbol{h}}_1 \\ \boldsymbol{b}_{21} & \boldsymbol{b}_{22} & \boldsymbol{c}_{21} & \boldsymbol{c}_{22} & \tilde{\boldsymbol{h}}_2 \end{bmatrix} \odot \begin{bmatrix} \boldsymbol{F}_1^H/\mu \\ \boldsymbol{F}_2^H/\mu \\ \boldsymbol{T}_1^H/\mu \\ \boldsymbol{T}_2^H/\mu \\ \boldsymbol{E}^\infty/\mu \end{bmatrix}, \tag{3}$$

where $\boldsymbol{F}^H$ are the hydrodynamic forces, $\boldsymbol{T}^H$ are the hydrodynamic torques, $\boldsymbol{E}^\infty$ is the strain rate tensor at infinity. The quantities $\boldsymbol{a}$, $\boldsymbol{b}$, $\boldsymbol{c}$, $\boldsymbol{g}$ and $\boldsymbol{h}$ are called mobility tensors and $\bigodot$ is the contraction on the larger number of indices possible. In the case of an external simple shear flow, we have:

$$\boldsymbol{u}^\infty(\boldsymbol{x}) = \dot{\gamma}(y - y_0)\hat{\boldsymbol{e}}_1 \tag{4}$$

In the case of inertia-free particles, the hydrodynamic forces and torques are given respectively by:

$$\boldsymbol{F}^H = -\boldsymbol{F}^{NH} \tag{5}$$

$$\boldsymbol{T}^H = -\boldsymbol{T}^{NH}, \tag{6}$$

where $\boldsymbol{F}^{NH}$ and $\boldsymbol{T}^{NH}$ are respectivelly the non-hydrodynamic forces and torques. In the present model, non-hydrodynamic forces and torques acting on the particles arise from dipole-dipole magnetic interactions. For the test particle 2, the magnetic force and torque are given respectively by:

$$\boldsymbol{F}_2^M = \frac{\mu_0 m_0^2}{4\pi r^4}\left[(\hat{\boldsymbol{p}}_1 \cdot \hat{\boldsymbol{p}}_2)\,\hat{\boldsymbol{r}} + (\hat{\boldsymbol{p}}_1 \cdot \hat{\boldsymbol{r}})\,\hat{\boldsymbol{p}}_2 + (\hat{\boldsymbol{p}}_2 \cdot \hat{\boldsymbol{r}})\,\hat{\boldsymbol{p}}_1 - 5\,(\hat{\boldsymbol{p}}_1 \cdot \hat{\boldsymbol{r}})\,(\hat{\boldsymbol{p}}_2 \cdot \hat{\boldsymbol{r}})\,\hat{\boldsymbol{r}}\right] \tag{7}$$

$$\boldsymbol{T}_2^M = \frac{3\mu_0 m_0^2}{4\pi r^3}\left[-\frac{1}{3}\hat{\boldsymbol{p}}_2 \wedge \hat{\boldsymbol{p}}_1 + (\hat{\boldsymbol{p}}_2 \wedge \hat{\boldsymbol{r}})\,(\hat{\boldsymbol{p}}_1 \cdot \hat{\boldsymbol{r}})\right], \tag{8}$$

where μ_0 is the magnetic permeability of the free space, m_0 is the magnetic dipole moment of the particles, $\hat{\boldsymbol{r}} = \boldsymbol{r}/r$ is the normalized relative distance. For the nondimensionalization of the set of equations representing the two-particle model here, we use the following appropriated scales:

$$|\boldsymbol{x}| \sim a \tag{9}$$

$$t \sim \dot{\gamma}^{-1} \tag{10}$$

$$|\boldsymbol{F}| \sim 6\pi\mu\dot{\gamma}a^2 \tag{11}$$

$$|\boldsymbol{T}| \sim 8\pi\mu\dot{\gamma}a^3 \tag{12}$$

Substituting the dimensional variables by the nondimensional ones, the expressions for the magnetic forces and torques written in terms of non-dimensional quantities result, respectively, in

$$\boldsymbol{F}_2^M = \frac{\alpha}{r^4}\left[(\hat{\boldsymbol{p}}_1\cdot\hat{\boldsymbol{p}}_2)\,\hat{\boldsymbol{r}} + (\hat{\boldsymbol{p}}_1\cdot\hat{\boldsymbol{r}})\,\hat{\boldsymbol{p}}_2 + (\hat{\boldsymbol{p}}_2\cdot\hat{\boldsymbol{r}})\,\hat{\boldsymbol{p}}_1 - 5\,(\hat{\boldsymbol{p}}_1\cdot\hat{\boldsymbol{r}})\,(\hat{\boldsymbol{p}}_2\cdot\hat{\boldsymbol{r}})\,\hat{\boldsymbol{r}}\right] \tag{13}$$

$$\boldsymbol{T}_2^M = \frac{3\alpha}{4r^3}\left[-\frac{1}{3}\hat{\boldsymbol{p}}_2\wedge\hat{\boldsymbol{p}}_1 + (\hat{\boldsymbol{p}}_2\wedge\hat{\boldsymbol{r}})\,(\hat{\boldsymbol{p}}_1\cdot\hat{\boldsymbol{r}})\right], \tag{14}$$

where

$$\alpha = \frac{\mu_0 m_0^2}{8\pi^2\mu a^6\dot{\gamma}}. \tag{15}$$

Physically, the parameter α gives the strenght of dipole-dipole magentic interaction for both force and torque. In particular, this parameter measures the relative importance between the magnetic effects from dipole-dipole interaction compared to the viscous effect on the particle trajectories.

In order to solve the equations of movement of the particles we use a fourth order Runge-Kutta scheme with an adaptive time step. We used three different mobility regions: far-field interactions, near field interactions and an intermadiate matching region for the shear mobilities. In this intermediate region we used an fifth order polynomial interpolation in r^{-1} of the numerical data of the analytic solution for the problem of two spheres by Lin *et al.* (1970), the same used by Cunha and Hinch (1996). The expressions for the far-field and near-field mobilities are given in Kim and Karrila (2013).

3. RESULTS AND DISCUSSION

We have examined two types of trajectories in particle collision in simple shear. Irreversible open trajectories called dispersive ones and closed irreversible trajectories called aggregative ones. Dispersive trajectories are the ones in which the moving particle has a net displacement across the streamlines after particle collision. This characterize a mixing process in a suspension quantified by a hydrodynamic particle diffusivity. In contrast, aggregative trajectories are the ones in which the moving particle forms a doublet with the reference particle. This corresponds to an aggregative process with a certain probability or rate to occur. In this work we have investigated how viscous hydrodynamic interactions and magnetic effects can change the relative frequency of aggregative and dispersive trajectories after particle collision in a shearing dilute suspension. A related problem in the context of sedimentation has been developed by Cunha and Couto (2011). Typical irreversible relative trajectories resulting in particle aggregation and dispersion are shown in Figure 1 (a) and (b). From a set of the irreversible closed trajectories the rate of particle aggregation can be evaluated whereas particle diffusivities are calculated based on the open irreversible trajectories with a net displacement.

In order to illustrate qualitatively the dispersiveness of the particles, a scatter diagram of the relative particle trajectories is explored. Actually, this diagram consists in the plot of all final positions of a beam of particles coming from a certain initial plane with a fixed initial orientation for the two particles. Figure 2 shows the scatter diagrams for $\alpha = 0.5$ and $x^{-\infty} = -20$.

The asymmetry in Figure 2-b is a direct consequence of non-symmetrical initial conditions for particle orientation. Aggregative trajectories are not displayed on the diagram, due to the fact that they never cross the infinity planes.

Now, in order to explore the interplay between aggregative and dispersive trajectories, we show the aggregative region for a given initial orientation of the particles. We define such regions as a basin of aggregation or in other words it corresponds to a drainage region of aggregative trajectories. Figure 3 shows the aggregative region for a $x^{-\infty} = -20$, $\alpha = 0.5$ and initial orientations $\hat{\boldsymbol{p}}_1^{-\infty} = (1,0,0)$ and $\hat{\boldsymbol{p}}_2^{-\infty} = (1/\sqrt{2}, 1/\sqrt{2}, 0)$. Due to the strong sensibility of the problem with respect to its initial conditions, it can be seen that the aggregation area appears to be very complex. By looking at Figure 3(b) and 3(c), some structures in the basin of aggregation appear to show some kind of self-similarity, indicating the possibility of existence of a fractal behavior. This kind of fractal behavior is common in the basins of attraction of non-linear dynamical systems.

By the numerical simulations of the trajectories, we can calculate a self-diffusivity coefficient for a test particle by integrating over all dispersive trajectories. The expression for the shear-induced hydrodynamic self-diffusivity is expressed as:

$$\boldsymbol{\mathcal{D}}^S = \dot{\gamma}a^2\phi\boldsymbol{f}^S(\alpha), \tag{16}$$

where $\boldsymbol{f}^S(\alpha)$ is given by Cunha and Hinch (1996):

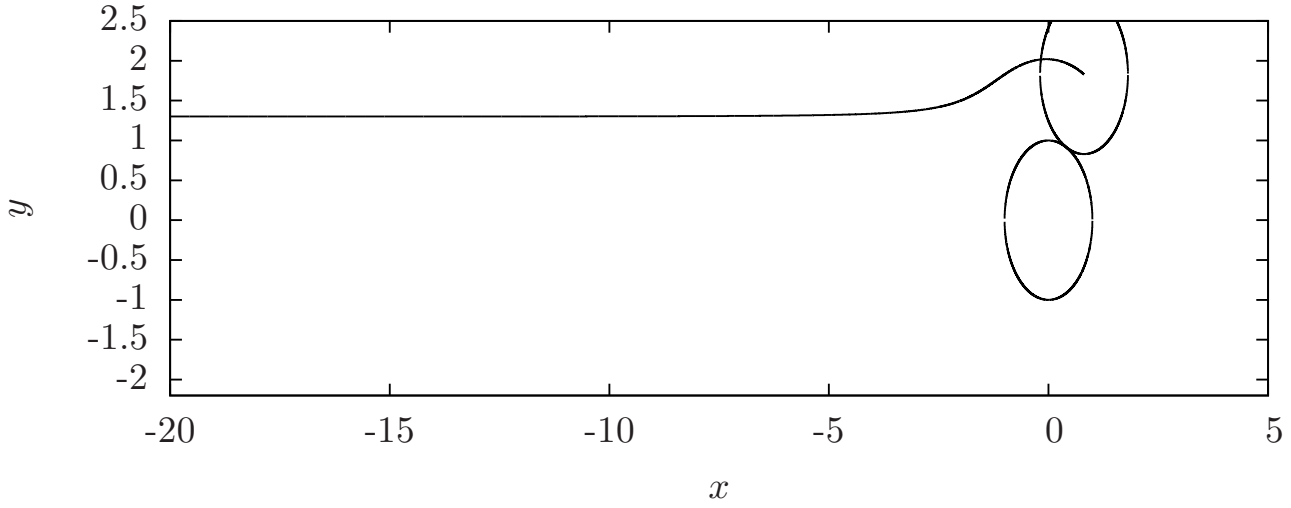

(a) Aggregative trajectory

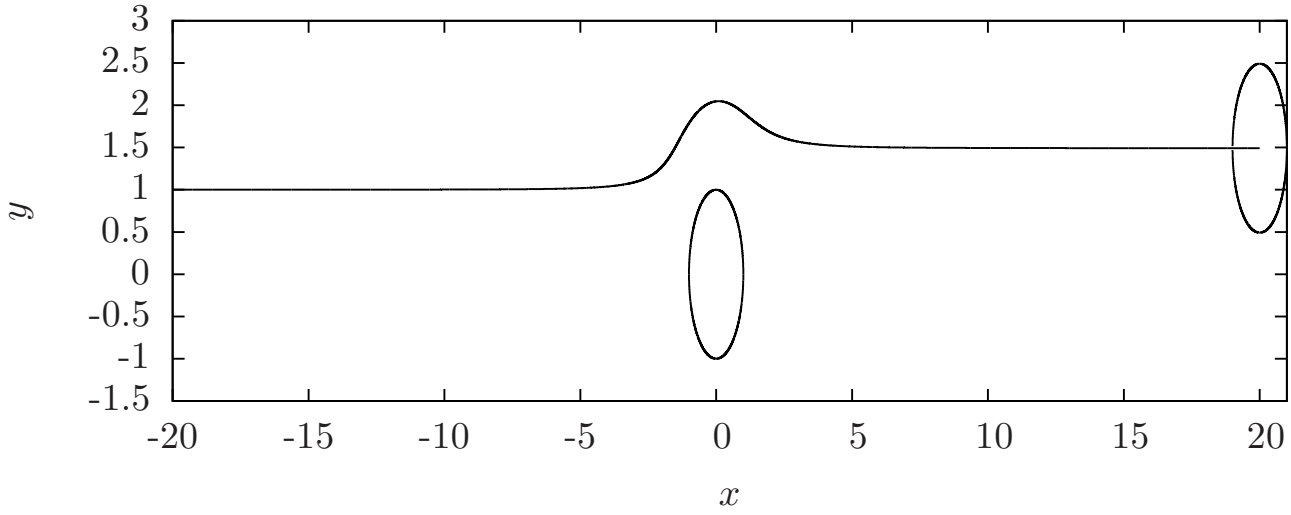

(b) Dispersive trajectory

Figure 1: Typical particle trajectories for spherical magnetic particles for $\alpha = 0.5$. Figure (a) has a starting position $\boldsymbol{r}^{-\infty} = (-10, 1.3, 0)$ with initial orientations $\hat{\boldsymbol{p}}_1^{-\infty} = (1, 0, 0)$ and $\hat{\boldsymbol{p}}_2^{-\infty} = (1/\sqrt{2}, 1/\sqrt{2}, 0)$. Figure (b) has a starting position $\boldsymbol{r}^{-\infty} = (-20, 1, 0)$ with the same initial orientations of (a).

$$\boldsymbol{f}^S(\alpha) = \left[\frac{3}{8\pi}\int_\Omega \Delta\boldsymbol{X}\Delta\boldsymbol{X}|y^{-\infty}|d\Omega\right] \tag{17}$$

For the case of magnetic particles with dipole moments, we have $d\Omega$ given by:

$$d\Omega = d\mathcal{P}_{\hat{\boldsymbol{p}}_1} d\mathcal{P}_{\hat{\boldsymbol{p}}_2} dA^{-\infty}, \tag{18}$$

where $\mathcal{P}_{\hat{\boldsymbol{p}}_k}$ is the probability for the particle to have its dipole moment orientation given by $\hat{\boldsymbol{p}}_k$. Thus, we have the expression for $d\mathcal{P}_{\hat{\boldsymbol{p}}_k}$ in terms of the probability density $P_{\hat{\boldsymbol{p}}_k}$:

$$d\mathcal{P}_{\hat{\boldsymbol{p}}_k} = P_{\hat{\boldsymbol{p}}_k} d\hat{\boldsymbol{p}}_k = P_k(\theta_k, \varphi_k)\sin(\theta_k) d\theta_k d\varphi_k, \tag{19}$$

where we used a spherical coordinate parametrization. For large separations, we have an uniform probability density for the orientations, given by:

$$P_k(\theta_k, \varphi_k) = \frac{1}{4\pi} \tag{20}$$

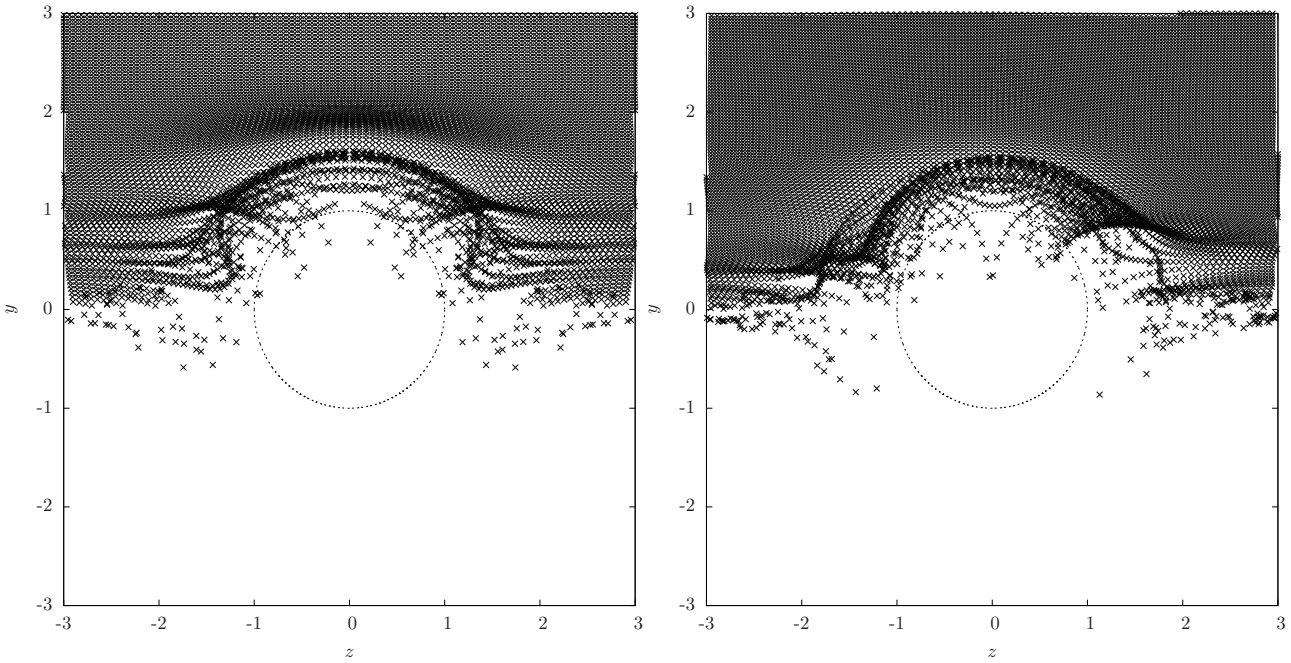

(a) $\hat{\boldsymbol{p}}_2^{-\infty} = (1/\sqrt{2}, 1/\sqrt{2}, 0)$ (b) $\hat{\boldsymbol{p}}_2^{-\infty} = (1/\sqrt{3}, 1/\sqrt{3}, 1/\sqrt{3})$

Figure 2: Scatter diagrams for $\alpha = 0.5$, $x^{-\infty} = -20$ and $\hat{\boldsymbol{p}}_1^{-\infty} = (1, 0, 0)$

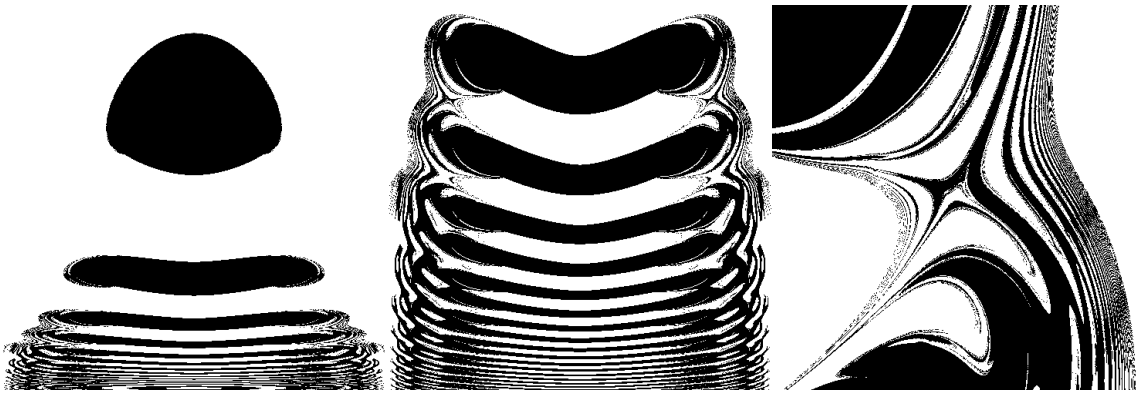

(a) (b) (c)

Figure 3: Detail of a section of the basin of aggregation for $\alpha = 0.5$. The black region represents the aggregative area on the collisional plane for a given pair of initial orientations. Figure (a) shows the region in which $z \in [-2.6, 2.6]$ and $y \in [10^{-3}, 1.4]$. (b) shows the region in which $z \in [-2.6, 2.6]$ and $y \in [10^{-3}, 0.3]$. (c) shows the detailed zoom of the region in which $z \in [1.2, 2.4]$ and $y \in [0.2, 0.25]$

Therefore, equation (17) becomes

$$\boldsymbol{f}^S(\alpha) = \frac{3}{8\pi}\frac{1}{16\pi^2}\int_{A_{disp}} dA^{-\infty}\int_{S^2} d\hat{\boldsymbol{p}}_1\int_{S^2} d\hat{\boldsymbol{p}}_2 \Delta\boldsymbol{X}\Delta\boldsymbol{X}|y^{-\infty}|, \tag{21}$$

where S^2 is the surface of an unit sphere and A_{disp} is the dispersive area. In order to evaluate the numerical value of the integral, we use the method of Monte-Carlo integration, in which the integral is approximated by:

$$\boldsymbol{f}^S(\alpha) \approx \frac{3}{8\pi}\frac{A^{-\infty}\pi^2}{4N}\sum_{k=1}^{N} \Delta\boldsymbol{X}_k\Delta\boldsymbol{X}_k|y_k^{-\infty}|\sin(\theta_1)\sin(\theta_2)\mathbb{I}_{A_{disp}}, \tag{22}$$

where $\mathbb{I}$ is the indicator function, given by:

$$\mathbb{I}_A = \begin{cases} 1 & \text{if } x \in A \\ 0 & otherwise \end{cases} \tag{23}$$

The results for the self-diffusivities obtained by the Monte-Carlo integration are shown in Figure 4. For small values of α we were able to compare our numerical results with the theory of Cunha and Hinch (1996). By a numerical fitting of our computational resuls, we found that for $\varepsilon = \alpha^{5/4}$ there is a linearity between the self diffusivity and $\delta^4 = \varepsilon^{0.4374}\left(\log(1/\varepsilon) + 1.347\right)^{-0.7012}$, as shown in the insert of Figure 4.

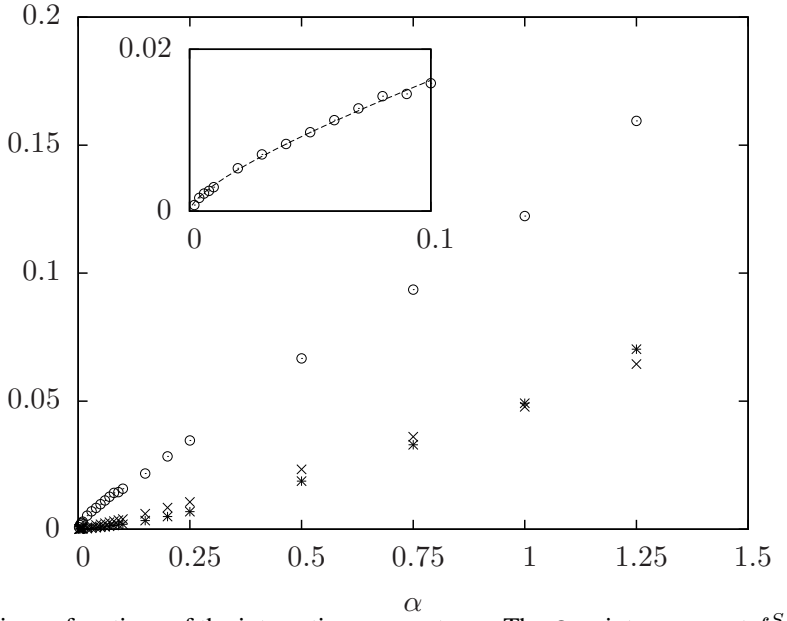

Figure 4: Self-diffusivities as functions of the interaction parameter α. The $\odot$ points represent f^S_{yy}, the $*$ points represent f^S_{zz}, $\times$ points are f^S_{yz}. The insert shows the comparison of the self diffusivities for small values of α with the theory of Cunha & Hinch. The dashed line is the function $0.1564\ \delta^4(\alpha)$.

It is important to note that the non-diagonal terms of the self diffusivity tensor do not vanish. Acually, the values for f_{yz} and f_{zz} have the same order. This is due to the fact that the net displacements of the trajectories in the y and z directions are not unconrrelated.

In the paper of Cunha & Hinch, the self-diffusivities in the $z-$direction are linear with ε. For small values of α, the diffusivity in the $z-$direction f^S_{zz} is linear with $\alpha^{5/4}$, as shown in Figure 5.

In a dilute homogeneous suspension, with a negligible number of aggregates, the rate of doublet formation is given by:

$$\frac{dN_2}{dt} = n_1 N_1 \dot{\gamma} a^3 J_{11}, \tag{24}$$

where J_{11} is given by the integral

$$J_{11} = \frac{1}{16\pi^2}\int_{A^{-\infty}} dA^{-\infty} \int_{S^2} d\hat{\boldsymbol{p}}_1 \int_{S^2} d\hat{\boldsymbol{p}}_2 |y^{-\infty}| \mathbb{I}_{\Omega_{agg}}. \tag{25}$$

Now, we perform a scaling argument in order to predict the type of dependence of J_{11} with respect to α. By equation (25), it is easy to see that J_{11} is linear with the nondimensional area $\tilde{A}_{agg}$, which is a "standard" nondimensional aggregative area. The aggregative area depends on the characteristic length ℓ in a way that

$$A_{agg} \propto \ell^2. \tag{26}$$

The lengthscale ℓ is related to the strength of dipolar interactions between the particles. In this context, we define ℓ as being the scale on which the hydrodynamic forces balance the magnetic dipolar forces. When this balance occurs, we have $F_H \sim F_M$, where $F_H \sim 6\pi\mu a U$ and $F_M \sim \frac{3\mu_0 m_0^2}{4\pi\ell^4}$. Balancing both effects, we find ℓ to be given by:

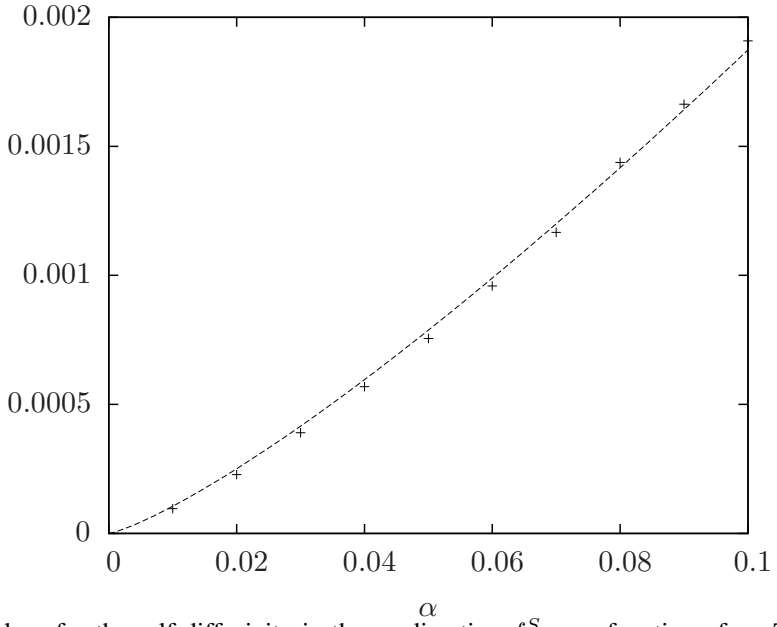

Figure 5: Numerical values for the self-diffusivity in the $z-$direction f_{zz}^{S} as a function of α. The dashed curve is the function $0.0333\ \alpha^{5/4}$.

$$\ell \sim a\alpha^{1/4}. \tag{27}$$

Therefore, we have:

$$J_{11} \propto \alpha^{1/2}. \tag{28}$$

Thus, this simple scaling argument suggests a square root dependence of J_{11} on α.

For the numerical computation of J_{11}, we perform a Monte-Carlo integration of the integral in (25). The results for this integration are shown in Figure 6.

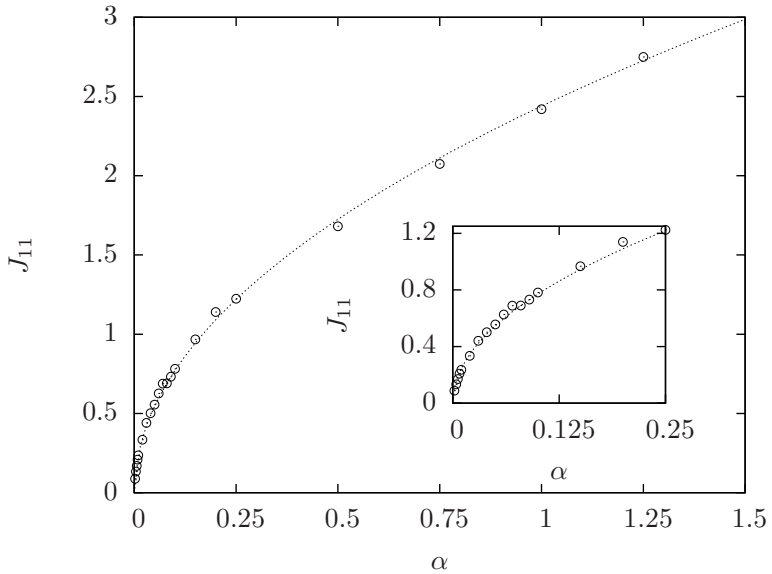

Figure 6: Numerical values for J_{11} as function of the interaction parameter α. The dashed line is the fit function $A\alpha^{1/2}$, where the parameter $A = 2.43896$ was obtained by a numerical fit.

The result shown in Figure 6 indicate the existence of a quite good quantitative agreement between our prediction by dimensional analysis and the numerical results by the Monte-Carlo method.

4. CONCLUSION

In this work, we have examined open and closed irreversible trajectories after collision of two interacting magnetic particles on a simple shear flow. Using the numerical simulations, we were able to investigate the interplay between aggregative and dispersive trajectories. Based on particle trajectory analysis we have computed self-diffusivities and the rate of particle aggregation for a dilute magnetic suspension with particles interacting hydrodynamically and magnetically. These macroscopic quantities are plotted as a function of the strength of the dipole-dipole magnetic interaction which measures the relative importance between magnetic particle interaction in comparison with viscous effects in the suspension, including hydrodynamic interaction.

The self-diffusivities and the rate of particle aggregation were found to be increasing functions of the magnetic parameter α. By comparing the $\mathcal{O}(\phi)$ of the self-diffusivity of magnetic particles for small values of α with those of non-magnetic rough particles (Cunha and Hinch, 1996) for small values of roughness ε, we have seen that the values for the self-diffusivities are slightly greater for the case of rough particles. For instance, taking a value of roughness $\varepsilon = 4 \times 10^{-2}$, the dimensionless $\mathcal{O}(\phi)$ self-diffusivity is calculated as being approximately 0.015, while for the same value of α, the self-diffusivity is given approximately by 0.008. The value of α which gives the same value for the self-diffusivity as $\varepsilon = 4 \times 10^{-2}$ is $\alpha \approx 9 \times 10^{-2}$. In the asymptotic limit for small α we determined that: $D^S_{yy} = \dot{\gamma} a^2 \phi f_{yy}(\alpha)$, with $f_{yy}(\alpha) \approx 0.1564\ \alpha^{0.5467} \left(\frac{5}{4}\log(1/\alpha) + 1.347\right)^{-0.7012}$, according to a theoretical prediction for a arbitrary small parameter breaking time-reversibility of particle trajectories (Cunha and Hinch, 1996). In addition, the rate of doublet formation is predicted as being $dN_2/dt = n_1 N_1 \dot{\gamma} a^3 J_{11}$, with $J_{11} = 2.4389\ \alpha^{1/2}$.

5. ACKNOWLEDGEMENTS

This work was supported by the Brazilian funding agencies CNPq - Ministry of Science, Technology and Innovation of Brazil (Grants: #402371/2013-5; #305764/2015-2; #441340/2014-8). GARN also wish to acknowledge CNPq for supporting him with a scholarship during this work at University of Brasilia-Brazil.

6. REFERENCES

Batchelor, G.K. and Green, J.T., 1972. "The determination of the bulk stress in a suspension of spherical particles to order c 2". *Journal of Fluid Mechanics*, Vol. 56, No. 03, pp. 401–427.

Cunha, F.R. and Couto, H.L.G., 2008. "Transverse gradient diffusion in a polydisperse dilute suspension of magnetic spheres during sedimentation". *Journal of Physics: Condensed Matter*, Vol. 20, No. 20, p. 204129.

Cunha, F.R. and Couto, H.L.G., 2011. "On the influence of the hydrodynamic interactions on the aggregation rate of magnetic spheres in a dilute suspension". *Journal of Magnetism and Magnetic Materials*, Vol. 323, No. 1, pp. 77–82.

Cunha, F.R., Gontijo, R.G. and Sobral, Y.D., 2013. "Symmetry breaking of particle trajectories due to magnetic interactions in a dilute suspension". *Journal of Magnetism and Magnetic Materials*, Vol. 326, pp. 240–250.

Cunha, F.R. and Hinch, E.J., 1996. "Shear-induced dispersion in a dilute suspension of rough spheres". *Journal of Fluid Mechanics*, Vol. 309, pp. 211–223.

Grandchamp, X., Coupier, G., Srivastav, A., Minetti, C. and Podgorski, T., 2013. "Lift and down-gradient shear-induced diffusion in red blood cell suspensions". *Physical review letters*, Vol. 110, No. 10, p. 108101.

Kim, S. and Karrila, S.J., 2013. *Microhydrodynamics: principles and selected applications*. Courier Corporation.

Lin, C.J., Lee, K.J. and Sather, N.F., 1970. "Slow motion of two spheres in a shear field". *Journal of Fluid Mechanics*, Vol. 43, No. 01, pp. 35–47.

Loewenberg, M. and Hinch, E.J., 1997. "Collision of two deformable drops in shear flow". *Journal of Fluid Mechanics*, Vol. 338, pp. 299–315.

7. RESPONSIBILITY NOTICE

The authors is are the only responsible for the printed material included in this paper.